Food Chemistry: X 25 (2025) 102162

Contents lists available at ScienceDirect

Food Chemistry: X

journal homepage: www.sciencedirect.com/journal/food-chemistry-x

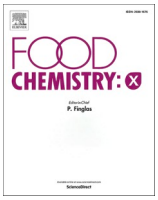

In situ quantification of fungicide residue on wheat leaf surfaces using matrix-assisted laser desorption/ionization time-of-flight mass spectrometry imaging technology

Xuerui Yang [a,b,c], Mengyao Shi [a], Minghui Hong [d], Zhixin Hui [a], Jiaqi Pan [a], Guangli Xiu [a,b,c], Lei Zhou [a,b,c,*]

[a] State Environmental Protection Key Lab of Environmental Risk Assessment and Control on Chemical Processes, School of Resources & Environmental Engineering, East China University of Science and Technology, Shanghai 200237, China
[b] Shanghai Environmental Protection Key Laboratory for Environmental Standard and Risk Management of Chemical Pollutants, School of Resources & Environmental Engineering, East China University of Science and Technology, Shanghai 200237, China
[c] Shanghai Institute of Pollution Control and Ecological Security, Shanghai 200092, China
[d] Nanjing Institute of Environmental Science, Ministry of Environmental Protection of China, Nanjing 210042, China

ARTICLE INFO

Keywords:
Leaf
Matrices
Metrafenone
Pesticide
Sublimation spraying

ABSTRACT

To overcome the time-consuming off-site limitations in conventional pesticide detection, this contribution presents an in situ quantitative analysis detection strategy for pesticides on leaf surfaces using matrix-assisted laser desorption/ionization time-of-flight mass spectrometry imaging technology. Taking fungicide metrafenone as a representative, we initially screened seven commonly used matrices, and identifying α-cyano-4-hydroxycinnamic acid as the most effective one in positive mode. Subsequently, coating the matrix using sublimation spraying method resulted in the highest mass intensity. The optimal combination of operation parameters were established with imaging step size of 30 μm × 30 μm, laser diameter of 75 μm, and laser energy of 4.01 μJ/pulse. Under these conditions, a lowest detection limit of 0.6 ng/mm^2 was reached for metrafenone, demonstrating extremely high sensitivity and strong repeatability. This method exhibits great potential for the analysis of various pesticides, including triadimefon and tebuconazole, thereby offering innovative approaches to the analysis of pesticide residues.

1. Introduction

The widespread use of agricultural pesticides has become a global concern due to their persistence in the environment and potential risks to human health and ecosystems (Maggi et al., 2023; Zhao et al., 2023). Pesticides, particularly fungicides, are commonly detected in the atmosphere, soil, water bodies, and agricultural products, raising significant concerns to food safety, environmental contamination, and public health (Chen et al., 2023; Zhao et al., 2023). Consequently, stricter regulations have been imposed by organizations such as the World Trade Organization (WTO) and the International Organization for Standardization (ISO) to monitor pesticide usage and set residue limits (Rani et al., 2021). Leaves, as the primary receptors of pesticide application, are crucial surfaces for detecting pesticide residues. Therefore, detecting pesticide residues on plant surfaces, particularly leaves, is crucial for assessing their environmental impact and ensuring compliance with safety standards (Li, 2022).

Currently, traditional destructive methods have been widely used for pesticide detection from plant surfaces. These methods include spectroscopic techniques (e.g., UV–Vis), chromatography, and chromatography-mass spectrometry (Feng et al., 2020; Pang et al., 2020; Wang et al., 2022). Although these methods are effective for both qualitative and quantitative analysis, they typically require sample extraction and preparation, which may result in sample loss and are time-consuming. Additionally, these methods may also have limitations in sensitivity when detecting pesticides at trace levels, and the extraction process itself is often time-consuming and labor-intensive (Ridha et al., 2024; Semysim et al., 2024; Yao et al., 2014). Due to their

* Corresponding author at: State Environmental Protection Key Lab of Environmental Risk Assessment and Control on Chemical Processes, School of Resources & Environmental Engineering, East China University of Science and Technology, Shanghai 200237, China.
E-mail addresses: yangxuerui@ecust.edu.cn (X. Yang), zhoulei@ecust.edu.cn (L. Zhou).

https://doi.org/10.1016/j.fochx.2025.102162
Received 21 February 2024; Received in revised form 2 January 2025; Accepted 4 January 2025
Available online 6 January 2025

destructive nature, these methods are unsuitable for on-site or in-situ monitoring of pesticide residues, highlighting the need for more efficient and non-invasive techniques.

To overcome these limitations, non-destructive methods such as Fourier Transform Infrared (FTIR) spectroscopy, Surface-Enhanced Raman Spectroscopy (SERS), and Near-Infrared (NIR) spectroscopy have been explored for real-time, non-invasive pesticide detection (Lv et al., 2024; Wang et al., 2021; Zhang et al., 2023). These techniques allow for direct analysis of pesticide residues on plant surfaces without altering the samples. However, while these methods are fast and offer non-destructive analysis, they often face sensitivity limitations, especially for detecting low concentrations of pesticides. Additionally, spatial distribution mapping of pesticide residues is challenging, as these techniques typically provide only surface-level or bulk concentration information without detailed spatial resolution (Shao et al., 2016; Villanueva et al., 2023).

In recent years, matrix-assisted laser desorption/ionization mass spectrometry (MALDI-MS) imaging has emerged as a powerful tool for the in situ, spatially resolved analysis of pesticide residues on plant surfaces. MALDI-MS can directly detect and map the distribution of pesticides without the need for complex pre-processing, making it ideal for studying pesticide behavior on plant surfaces. Previous studies have demonstrated the capability of MALDI-MS to detect various pesticides, such as thiram, imidacloprid, and propamocarb, on crops like banana and wheat (Annangudi et al., 2015; Wang et al., 2023). Despite its success in qualitative mapping, MALDI-MS has yet to provide reliable quantitative data, especially at the trace levels typically found in agricultural environments. Furthermore, the complexity of commercial pesticide formulations, which often contain adjuvants, presents additional challenges in achieving accurate and reproducible quantification.

To address this issue, this study aims to develop an optimized MALDI-TOF-MS imaging approach for the quantitative detection of pesticide residues, specifically the fungicide metrafenone (MF), on wheat leaves. MF was chosen as a model pesticide due to its widespread use and environmental persistence (Kamel & Hoppin, 2004; Pimmata et al., 2013). The objective is to optimize key experimental parameters, including matrix selection, matrix deposition techniques, and laser settings, to enhance the sensitivity and reproducibility of MALDI-TOF-MS for pesticide quantification. We hypothesize that by optimizing these parameters, MALDI-TOF-MS can achieve highly sensitive and accurate quantitative analysis of pesticide residues directly on plant surfaces. The findings of this study will provide valuable insights into the environmental risks associated with pesticide residues and offer a new methodology for assessing pesticide contamination in agricultural products.

2. Materials and methods

2.1. Reagents

Detailed reagents used in this work were shown in the Table S1, supplementary data, SD. The specific preparation method of the matrix was as follows. A 10 mg·mL^{-1} solution of CHCA and DHB was prepared by dissolving them in acetonitrile/H_2O (1:1, *v*/v). 9AA was dissolved in isopropyl alcohol/acetonitrile (1:1, v/v) to form a 1 mg·mL^{-1} solution. SA was dissolved in $CHCl_3$/acetonitrile (1:1, v/v) to form a 10 mg·mL^{-1} solution. NEDC, DAN, and THAP were dissolved in methanol/acetonitrile (1:1, v/v) to form a 1 mg mL^{-1} solution. After preparation, the solutions were sonicated for 30 min to ensure complete dissolution, and stored at low temperature.

2.2. Wheat cultivation

Wheat (*Triticum aestivum* L.) plants were cultivated under controlled environmental conditions in an artificial climate incubator. The growth substrate consisted of agricultural soil collected from field sites in Qingpu District, Shanghai, China (30°58′08″N, 121°01′56″E). Prior to germination, wheat seeds were surface-sterilized and subsequently imbibed in deionized water. The pre-treated seeds were then uniformly distributed on moistened germination paper and maintained until radicle protrusion was observed. When the coleoptiles reached approximately 1 cm in length, seedlings were transferred to the growth chamber maintained under a period regime of 14 h daytime and 10 h dark cycle. The specific parameters of the climate incubator are shown in Table S2. The wheat plants were grown to the containing-five-leaf stage to be utilized for subsequent experiment.

2.3. MALDI-TOF-MS imaging method for sample preparation

In the present work, wheat leaves exhibiting vigorous growth were selected and washed three times with ultrapure water to remove surface dust. By using the conductive tape, the wheat leaves were fixed on the indium-tin oxide (ITO) coated side of the conductive glass slides. Subsequently, the target MF solution was dropped on the surface of the wheat leaves and placed under dark conditions within a laboratory fume hood for 1 h duration. Following complete solvent evaporation, the samples were prepared for subsequent MALDI-TOF-MS imaging analysis. A commercial spray gun (Platinum 0.2, Chiyoda Japan Co., Ltd.) and the matrix elevating instrument (iMLayer™ Shimadzu China Co., Ltd) were utilized to apply a uniform coating of the matrix solution onto the sample surfaces. Such methodical matrix application was critical for enhancing ionization efficiency during mass spectrometric analysis. The detailed procedural protocols for the three matrix coating methods are comprehensively documented in the Text S1. Stereomicroscopy was performed to fully ascertain the coating uniformity of the samples. Subsequently, MALDI-TOF-MS imaging analysis was conducted utilizing predefined instrumental parameters, displayed in Fig. S1, supplementary data, SD. To enhance the signal-to-noise ratio and reduce potential variability, each experimental sample was replicated in duplicate. Detailed information about the instruments used during the experiment was displayed in Table S3.

The longitudinal distribution profile of MF permeation in wheat leaves was investigated using frozen sectioning technology. A series of MF standard solutions at varying concentrations were applied dropwise to the wheat leaf surfaces, followed by ambient air drying. After that, gelatin was dissolved in ultrapure water at a ratio of 1:9 (*w*/w) by heating to 40 °C in a water bath. Wheat leaf specimens containing MF were embedded and frozen in molds. After that, frozen samples were sectioned using a freezing microtome at −20 °C to a thickness of 60 μm. The sections were attached to conductive glass slides, sprayed with a matrix, and analyzed further using MALDI-TOF-MS imaging.

2.4. MALDI-TOF-MS imaging for data acquisition and analysis

The MALDI-TOF-MS imaging data acquisition system utilized SHIMADZU Imaging MS Solution ver. 1.30 software. Before each imaging data acquisition, the instrument was mass calibrated using the software. The regions of interest in the leaf were studied in both negative and positive modes sample and detector voltages of 3.00 and 1.75 kV, respectively. The obtained spectra were acquired at a speed of 1000 Hz over the mass range of *m/z* 100.00–500.00. Images of the compounds of interest were acquired manually using the root mean square normalization protocol in the software. Additional details are provided in the Table S4.

3. Results

3.1. Method optimization on MALDI-TOF-MS imaging by using selected MF fungicides as an example

3.1.1. Optimization of matrix

The identification performance of the MALDI-TOF-MS imaging technique was highly dependent on the selection of matrix chemicals, as

which played a critical role for the intensity of mass spectral signal and data interpretation. It was believed that an optimal matrix chemical possessed strong photon absorbance at the laser excitation wavelength, solubility in solvents compatible with the analytes, vacuum stability, and the capacity to promote ionization (Giampà et al., 2016; Ouyang, Wang, et al. (2024); Wang et al., 2013). Given the critical influence of the matrix on data quality and information recovery, several commonly utilized matrix chemicals were evaluated in this study for MF detection. These included α-cyano-4-hydroxycinnamic acid (CHCA), 2,5-dihydroxybenzoic acid (DHB), 9-aminoacridine (9AA), sinapic acid (SA), N-(1-naphthyl) ethylenediamine dihydrochloride (NEDC), 1,5-diaminonaphthalene (DAN) and 2,4,6-trihydroxyacetophenone (THAP). Their capacities to enable effective MF measurement by MALDI-TOF-MS imaging were systematically examined.

As background matrix signals could potentially interfere with the detection of the analytes of interest, experiments were initially performed in the absence of MF (Braga et al., 2019; Ouyang et al., 2023; Song et al., 2021). Matrix solutions were directly deposited onto the surface of wheat leaves followed by analysis using MALDI-TOF-MS imaging. Since the characteristic bromine-containing MF protonated isotope ions $[M + H]^+$ ions were observed at *m/z* 409.06 and 411.06 in positive ion mode, the imaging response of the matrix spots under the specific m/z was evaluated. As illustrated in Fig. 1, among the matrices evaluated, DHB and THAP exhibited signals at m/z 409.06 and 411.06, consistent with the expected MF isotope ions. Matrix spotting with SA generated a minor bright spot in the corresponding ion images, while CHCA, 9AA, NEDC and DAN displayed no detectable background interference at the noted *m/z* values in positive ion mode. These results demonstrated that DHB, THAP, and SA generated background interference consistent with the MF target ions, rendering them unsuitable as matrices for surface analysis.

Furthermore, the matrix solutions CHCA, 9AA, DAN, and NEDC were combined with the target MF, followed by MALDI-TOF-MS imaging. As shown in Fig. 2(B-1, B-2), all four matrices coated with MF displayed a clear signal (m/z = 407.05/409.05 ($[M - H]^-$)) response, except for the matrix NEDC where no ^{81}Br signal of MF was detected (m/z 409.05). Despite the effective ionization of MF by the CHCA, 9AA and DAN matrices in negative mode, the relative isotopic peak intensities deviated from theoretical abundances based on the natural isotopic distributions of ^{79}Br (50.69 %) and ^{81}Br (49.31 %) (Xu et al., 2021). Accordingly, the intensity of the ^{79}Br peak in the mass spectra would be slightly higher than that of ^{81}Br, as confirmed in a previous reported study (Hong et al., 2021). Since the peak intensity data in the negative ion mode were distorted, the results in the positive ion mode were relatively reliable. Consequently, the CHCA matrix in positive ionization mode was concluded to enable optimal ionization and accurate measurement of MF, providing a robust basis for further method optimization.

3.1.2. Optimization of spraying methods

In MALDI-TOF-MS imaging analysis, the spraying method of the matrix was critical for achieving homogeneous analyte-matrix co-crystals, which was the basis for obtaining high quality images of spatial distribution and quantitative reproducibility (Giampà et al., 2016; Wang et al., 2013). The matrix spraying methods could be classified as solvent-assisted methods, including direct dry drop and spray gun application, or solvent-free methodologies such as sublimation. The dry drop technique involved direct deposition of matrix solution onto the sample surface prior to imaging. The remaining two approaches was utilized a commercial spray gun or a matrix sublimation instrument to achieve homogeneous matrix coating over the analytical area. In this study, these three representative matrix spray methods were evaluated using a CHCA matrix and the results were illustrated in Fig. 3.

By utilization of the dry drop coating method, the results displayed the spatial distribution of MF on the leaves exhibiting incongruence with the original dispensed droplet shapes. It was a challenge to precisely locate the MF droplets after drying, and this method resulted in distortion of the spatial distribution of MF. Furthermore, under identical analytical parameters, significant variations in the MS signals or MF between experimental replicates were observed. The spray gun coating parameters, specifically the air flow and exhaust valve settings, were systematically optimized to achieve optimal spatial resolution and signal intensity. However, unexpectedly weak MF distributions were detected. This signal reduction was subsequently attributed to the displacement of MF by the impacting matrix droplets. In contrast, employing the matrix sublimation method demonstrated a distinct spatial distribution of MF on the leaf surface, characterized by well-defined droplets exhibiting high intensity mass spectral peaks and excellent reproducibility. The sublimation method does not require the addition of organic solvents, ensuring uniform matrix crystallization and controlling thickness of the matrix. These attributes facilitate reliable reproducibility of the analytical outcomes (Bodzon-Kulakowska et al., 2020) Based on the collective evidence, the sublimation deposition method employing a CHCA matrix emerged as the optimal approach. Additionally, the instrument parameters for MALDI-TOF-MS imaging will be optimized on this basis.

3.1.3. Optimization of MALDI-TOF-MS imaging instrument parameters

During data acquisition, MALDI-TOF-MS imaging software gridded the sample image into micron-sized pixel points, with an average MS map obtained for each pixel point. The final visualized image was attained by integrating and processing each MS data point (Balluff et al., 2021; Deininger et al., 2011; Fonville et al., 2012; Ouyang, Huang, et al. (2024)). During the actual operation, when the region of interest (ROI) of the sample was selected, the laser source remained stationary and the analysis was completed by the movement of the two-dimensional (2D) sample stage. Therefore, the pitch of the 2D stage in the X- and Y-axis directions determined the pixels size of the visualized image. According to the MALDI-TOF-MS setup, various pitches to measure MF on wheat leaves were determined (equal distance in X- and Y-axis directions), including 10 μm (pixels 62,500), 30 μm (pixels 21,010), 50 μm (pixels 7910), 70 μm (pixels 3901), 90 μm (pixels 2432) and 110 μm (pixels 1674). Optimization of the step size 2D platform movement step size was performed. As shown in Fig. 4(A), optimal delineation of the MF spatial distribution was attained at a pitch of 10 μm step size. It was evident that the image had the highest pixel value below 10 μm. However, a step size of 10 μm confines the definable analytical area to 2500 μm × 2500 μm, which proves insufficient to fully encompass the fungicide deposition area. The heatmap was blurred when the pitch was above 50 μm. Hence, 30 μm was defined as the optimal step size movement.

In alignment with previous findings (Chang et al., 2024; Dreisewerd et al., 1995), the analyte mass spectral signal response exhibited marked dependence on selected laser spot dimensions and pulse energy.

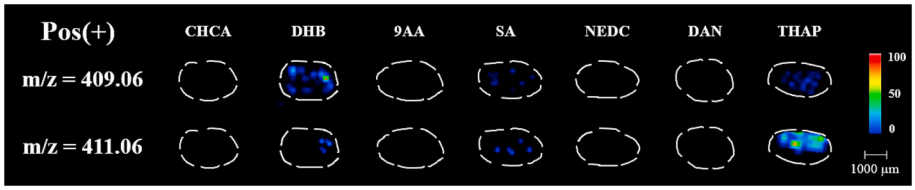

Fig. 1. MALDI-TOF-MS imaging of different matrices on blank wheat leaf at m/z = 409.06 and 411.06.

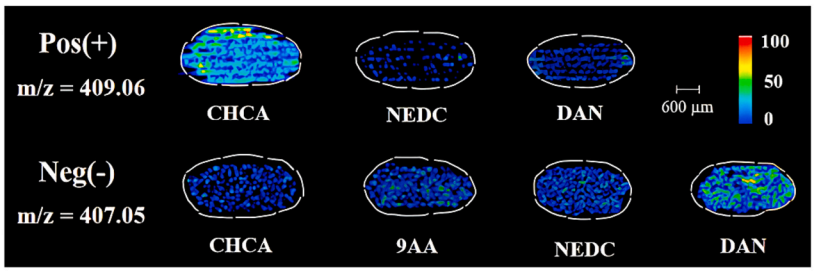

A

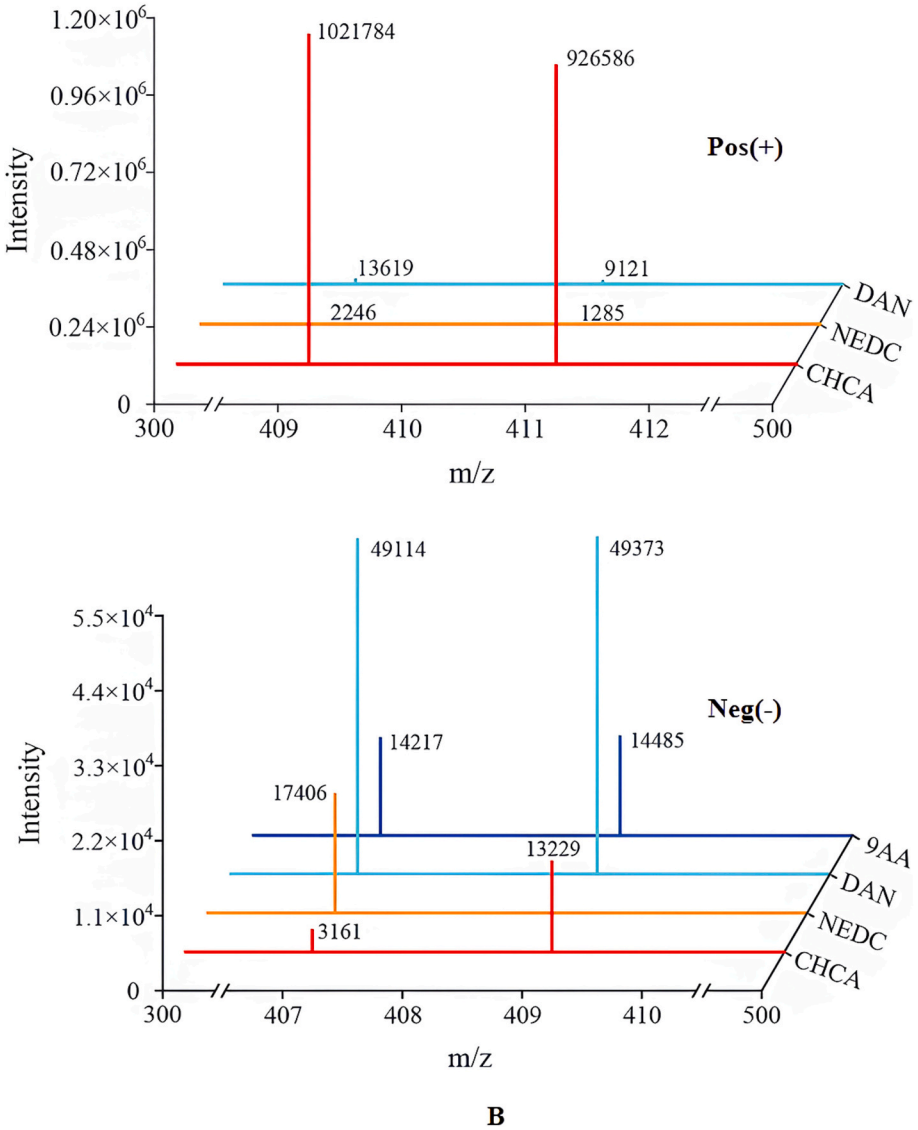

B

Fig. 2. (A) MALDI-TOF-MS imaging and (B) MS signal intensities (m/z = 409.06/411.06) of MF in various matrices in positive and negative ion modes (filtered matrix peaks).

Consequently, exploratory investigative optimization of these instrument parameters was conducted, and the results were presented in Fig. 4 (B) and Fig. S2. With an increase in laser spot diameter and energy, the obtained MF mass spectral signals appeared to follow a normal distribution, with the maximum intensity response attained utilizing a 75 μm beam diameter coupled to 71.0 % of the instrumental energy output, equally 4.01 μJ/pulse of laser energy. In the work of Chang et al. (2024), quasi-thermal desorption simulations were employed, and mass spectral signal intensities increased concomitantly with increasing laser pulse energies were verified. However, excessively large laser spots tended to suffer from "over-saturated" blurring. This was probably attributed to the onset of secondary processes, such as an increase in the number of collisions in the expanding particle plume and charge repulsion, leading to broadening and distortion of the mass spectral signal peaks and increased fragmentation.

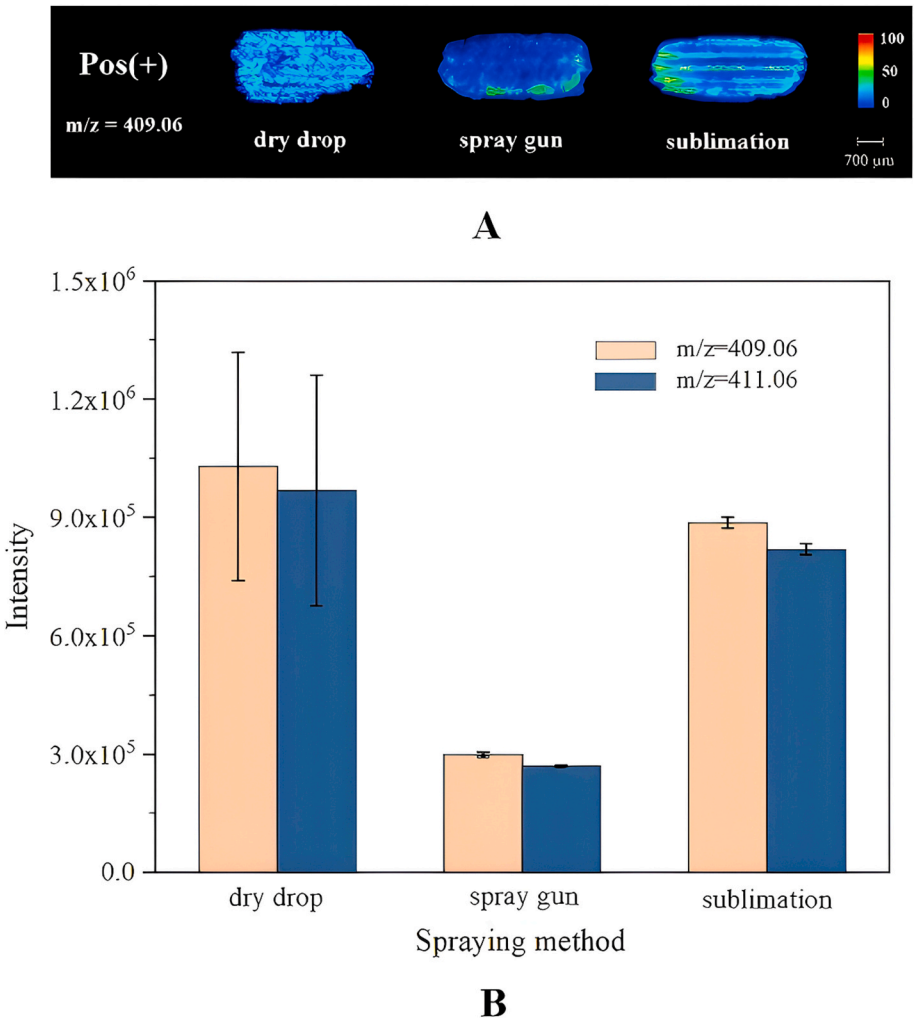

Fig. 3. (A) MALDI-TOF-MS imaging and (B) MS signal intensities (m/z = 409.06/411.06) of MF under various matrix spraying methods in positive ion mode with CHCA.

3.2. Quantitative detection of fungicide MF on wheat leaves

3.2.1. Limit of detection (LOD) and precision

Given the attenuating effects of rainfall, infiltration, and photodegradation the concentration of fungicides remaining on the surface of the leaves would mostly be at the trace levels, necessitating the higher sensitivity of the in situ detection MALDI-TOF-MS imaging method (Dolinová et al., 2004; Halle et al., 2006; Monadjemi et al., 2011). The limit of detection (LOD) was defined as minimum analyte level that enables reliable detection, constituting a critical analytical performance metric (Lepucki et al., 2021; Lux et al., 2022; Vicente et al., 2020). Under optimal instrumental conditions, a gradient series of low-concentration target MF solutions was configured to characterize the attainable LOD value. Specifically, 0.5 μL of MF solutions containing 0.4 ng, 2.0 ng, 4.0 ng, 6.0 ng and 8.0 ng were added dropwise to the surface of wheat leaves and dried for further detection. The MF mass spectra peak and thermogram signal could be observed with at a drop addition of 2.0 ng, as it was observed at 0.4 ng. These results were reliable, and reproducible across repetitive analyses under identical conditions, thus, establishing the LOD associated with the optimized method as 2.0 ng/drop, equivalent to 0.6 ng/mm^2 of MF. Relative to the in situ fungicide detection approach reported by Annangudi et al. (2015) with an LOD of 60.0 ng, the current optimized methodology enhances the sensitivity by 30 times, achieving an LOD of 2.0 ng. Notably, the European Food Safety Authority (EFSA) has implemented maximum residue limits (MRLs) for MF ranging from 0.01 to 2 mg/kg, depending on the specific crop. By using the MALDI-TOF-MS imaging technology, the limit of detection for MF on leaf surfaces was equivalent to 2 mg/kg of leaves.

Parallel repeatability assessments indicated five 2 μL MF aliquots at a concentration of 500 μM were deposited onto the wheat leaf surfaces, introducing an absolute deposition of 0.4 μg. The intensities of the recorded analyte signa demonstrated a relative standard deviation of 6.42 % across replicates. This minimal variability verifies the excellent quantitative reproducibility obtained using the optimized detection methodology.

3.2.2. Quantification range and recovery rate

Solutions containing 0.008 μg, 0.020 μg, 0.04 μg, 0.06 μg, 0.12 μg, 0.24 μg, 0.6 μg, 0.96 μg and 1.2 μg of MF were prepared to determine the quantitation range. Aliquots of 0.5 μL MF solution were deposited on wheat leaf surfaces and analyzed utilizing an optimized MALDI-TOF-MS imaging method, which employed a sublimator sprayed with matrix CHCA matrix at a thickness of 1.2 μm over a 30 μm × 30 μm step size using a 75 μm diameter laser at 4.01 μJ/pulse power. The linearity and quantitative range of MF using the optimized method were obtained, and the results were shown in Fig. 5. The R^2 value of the standard curve was observed to be 0.9934 for the MF mass range of 0.008–0.6 μg, indicating a direct linearity and demonstrating its usefulness for quantitative analysis.

Finally, a spiked recovery test was performed, in which MF solutions

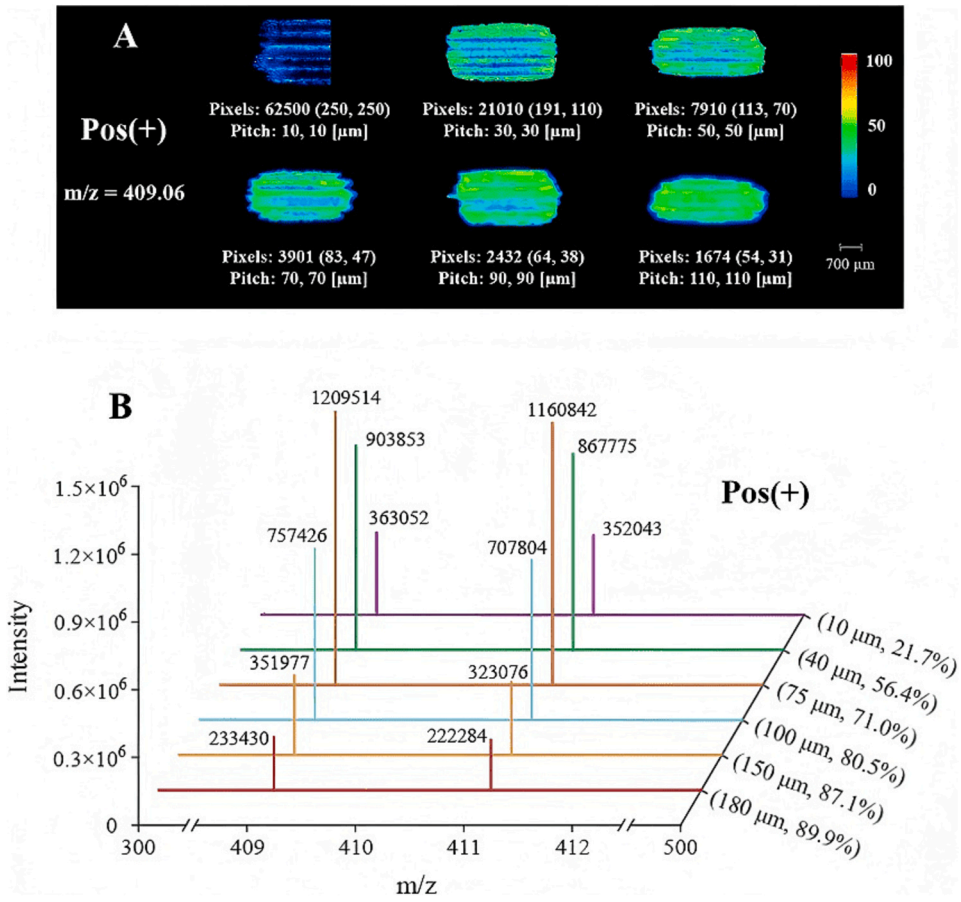

Fig. 4. (A) MALDI-TOF-MS imaging of MF at various pitches and (B) MS signal intensities (m/z = 409.06/411.06) of MF at different laser diameters and intensities using matrix sublimation method in positive ion mode with CHCA.

were added dropwise to the surface of wheat leaves at low, medium and high dosage (0.024 μg, 0.120 μg and 0.480 μg). Quantification was replicated six times at each concentration under identical instrumental parameters. As shown in Table 1, the average recovery was calculated as 97.75 ± 11.44 %.

3.3. Distribution characteristics of MF on wheat leaves

The distribution of fungicide on the crop after application was closely correlated with epidermal morphological features of the leaf. Scanning electron microscopy (SEM) was utilized here to resolve the micromorphological features of wheat foliar surfaces. The epidermis of leaves was observed with an ordered row of corrugated structures contoured around surface folds and clearly visible structures such as leaf hairs, stomatal apparatus and leaf slit (Fig. 6(A)). The target MF distribution was arranged in a linear, and compact manner, consistent with the path of the cell structure on the wheat leaf surface (Fig. 6(B)).

The MF concentration at the edge of the droplet was higher, consistent with microscopic observations made by Trivella and Richard (2014). Due to limitations in technology available at that time, only the microscope was used to photograph the apparent phenomenon. The accumulation of MF at the edges was caused by the “coffee ring effect”, where the evaporation rate was faster at the edges of MF droplets, forming a directional flow from the center to the edges of the droplets was formed to replenish the evaporated solvent at the edges (Deegan et al., 1997; Hu & Larson, 2006; Robert et al., 2000). Studies have the demonstrated that the inclusion of surfactants, such as lignin sulfonate, enables modulation of fungicide distribution uniformity across leaf surfaces, consequently improving crop protection efficacy (Hejazi, 2020; Monadjemi et al., 2011). In addition to profiling the foliar MF distribution, combined with the frozen section technique, the imaging of MF infiltrating into the leaf suture was observed using MALDI-TOF-MS imaging, as shown in Fig. 6(C)).

3.4. Feasibility of applying MALDI-TOF-MS imaging to the detection of common pesticides

In the present work, the potential application of MALDI-TOF-MS imaging for rapid in situ detection of agrichemical residues on crop surfaces was investigated, using the broad-spectrum fungicides triadimefon (TDF) and tebuconazole (TEB) as model compounds. Through systematic optimization of matrices, analytical step sizes, and instrumental parameters, an expeditious in-situ identification method for pesticides TEB and TDF on the surface of wheat leaves was constructed, as displayed in Table S5. As exemplified for TDF, shown in Fig. 7 and Fig. S3, 0.5 μL aliquots containing 20–30 ng deposited on leaves revealed well-defined molecular distribution images concordant with the acquisition of anticipated protonated TDF signals at m/z 294.10. Analogously, the thermogram signal and characteristic mass spectra at m/z 308.15 of pesticide TEB were rapidly imaged and recognized by MALDI-TOF-MS imaging technology (Fig. S4). Additionally, guided by the active ingredient concentration within the commercial TEB formulation, a 500 μM mimic suspension approximating field application levels was prepared in the laboratory. As shown in the Fig. 7, after applying the 1 μL droplets onto the wheat leaf surface, the images of TEB commercial aliquots were successfully captured. The present study demonstrated the utility of MALDI-TOF-MS imaging for the rapid screening of pesticides in both active ingredients and compounds present in commercial formulations. Unlike conventional pesticide residue analysis which relies on solvent extraction followed by GC or LC,

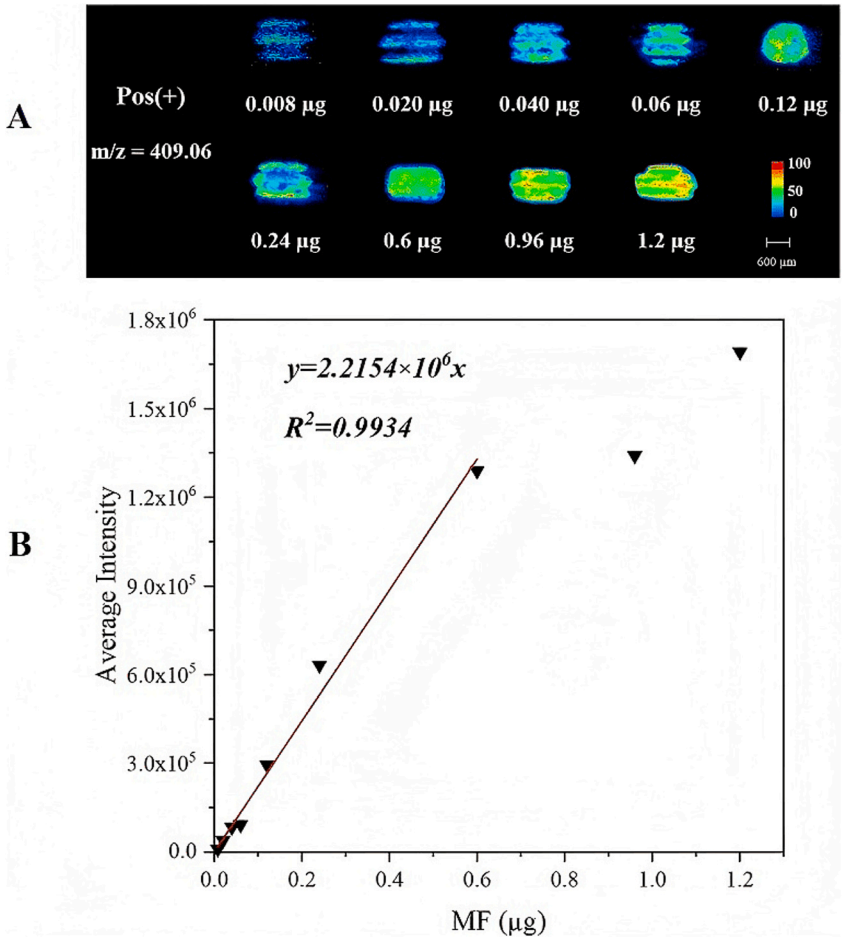

Fig. 5. (A) Determination of the minimum detection limit of MF on the wheat leaf surface using the matrix sublimation method in positive ion mode with CHCA. MALDI-TOF-MS imaging at various MF concentrations. (B) Linear relationship and quantitative range of MF obtained using MALDI-TOF-MS imaging.

Table 1
Results of MF sample recovery experiments on wheat leaf surface.

Addition amount (μg)	Recovery rate (%)	Average recovery rate (%)
0.024	100.83±6.85	
0.120	107.33 ±3.70	97.75 ± 11.44
0.480	87.50±2.74	

MALDI-TOF-MS imaging technology requires minimal sample pretreatment prior to direct analysis. By allowing in situ characterization and quantification of pesticide, this innovative technique provided new prospects for pesticide research.

4. Conclusion

This study confirmed the hypothesis that MALDI-TOF-MS can be optimized for in situ, quantitative analysis of pesticide residues, specifically metrafenone (MF) on plant surfaces. The conventional methodological approach to analyzing pesticide residues on leaf surfaces has been characterized by protracted experimental timelines and limited analytical depth. By using the MALDI-TOF-MS imaging technology, this research develops an innovative and expeditious quantitative detection methodology for pesticide residues on leaf surfaces. The proposed method addresses critical limitations of existing analytical protocols and substantially advances the capabilities of pesticide residue detection. This technological approach provides a robust and rapid analytical framework for detecting pesticide residues on the surfaces of agricultural produce. Moreover, it presents researchers with a novel investigative strategy for comprehensively understanding pesticide transformation mechanisms and spatial distribution dynamics on leaf interfaces. Main conclusions were as follows.

(1) **MALDI-TOF-MS Validation for Quantitative Detection.** This study confirmed the hypothesis that MALDI-TOF-MS can be optimized for in situ, quantitative analysis of pesticide residues, specifically metrafenone (MF) on plant surfaces. With optimized matrix selection and experimental conditions, a detection limit of 0.6 ng/mm^2 was achieved, demonstrating the potential for accurate pesticide quantification.
(2) **Matrix Optimization and Sensitivity Enhancement.** By screening seven matrices, CHCA was identified as the most effective for MF ionization, and sublimation spraying method could significantly improved the sensitivity.
(3) **Localization and Distribution Mapping.** Frozen section technique provided clear spatial mapping of MF on wheat leaf surfaces, confirming the ability of MALDI-TOF-MS to visualize pesticide distribution and penetration into plant tissues.
(4) **Application to Other Pesticides.** It was also demonstrated the possibility of MALDI-TOF-MS imaging for the detection of the remaining pesticides TEB, TDF, and commercial agricultural formulations.
(5) **Implications for Environmental Risk Assessment.** MALDI-TOF-MS imaging technology proved to be a valuable tool for the rapid detection of pesticides on leaf surfaces. The results obtained in this study provide a novel method for accurately evaluating the environmental risks of pesticides.

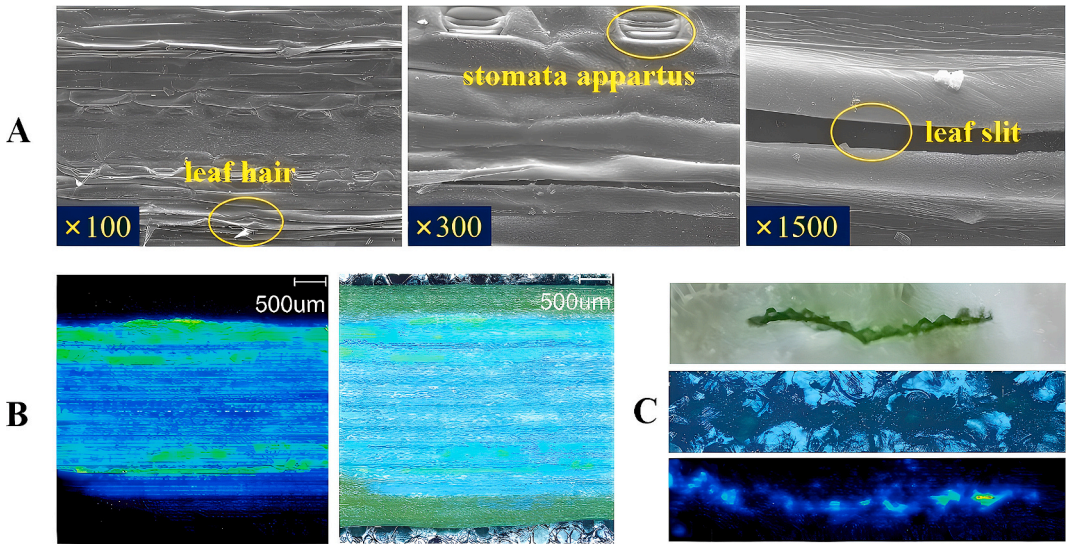

Fig. 6. (A) Microstructure of wheat leaves at different magnifications; (B) spatial distribution of MF on the surface of wheat leaves; (C) distribution of MF on the longitudinal section of wheat leaves (the following analytical imaging results: (1) a longitudinal cross-section of the embedded leaf specimen, (2) a pre-imaging visualization of the embedded leaf sample, and (3) a longitudinal pesticide distribution imaging outcome).

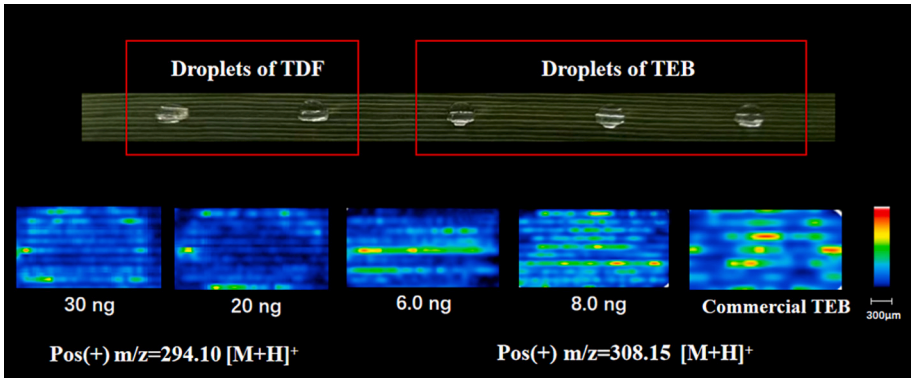

Fig. 7. MALDI-TOF-MS imaging of pesticide TDF, TEB and commercial TEB solution.

CRediT authorship contribution statement

Xuerui Yang: Writing – original draft, Validation, Investigation, Conceptualization. **Mengyao Shi:** Formal analysis. **Minghui Hong:** Resources, Investigation, Formal analysis. **Zhixin Hui:** Writing – review & editing. **Jiaqi Pan:** Methodology. **Guangli Xiu:** Project administration, Funding acquisition. **Lei Zhou:** Validation, Supervision, Funding acquisition.

Declaration of competing interest

The authors declare that they have no known competing financial interests or personal relationships that could have potentially influenced the work presented in this paper.

Data availability

Data will be made available on request.

Acknowledgements

The current study received financial support from the National Natural Science Foundation of China (No. 22306064 & 22176059), the Natural Science Foundation of Shanghai (23ZR1417500), and Fellowship of China Postdoctoral Science Foundation (2023M731085). We also thank Dr. Junling Dun from Analytical Applications Center, Shimadzu (China) Co., Ltd. for the technical support on MALDI-TOF analysis.

Appendix A. Supplementary data

Supplementary data to this article can be found online at https://doi.org/10.1016/j.fochx.2025.102162.

References

Annangudi, S. P., Myung, K., Avila Adame, C., & Gilbert, J. R. (2015). MALDI-MS imaging analysis of fungicide residue distributions on wheat leaf surfaces. *Environmental Science & Technology, 49*(9), 5579–5583. https://doi.org/10.1021/es506334y

Balluff, B., Hopf, C., Porta Siegel, T., Grabsch, H. I., & Heeren, R. M. A. (2021). Batch effects in MALDI mass spectrometry imaging. *Journal of the American Society for Mass Spectrometry, 32*(3), 628–635. https://doi.org/10.1021/jasms.0c00393

Bodzon-Kulakowska, A., Arena, R., Mielczarek, P., Hartman, K., Kozoł, P., Gibuła-Tarlowska, E., Wrobel, T. P., Gąsior, Ł., Polański, Z., Ptak, G. E., & Suder, P. (2020). Mouse single oocyte imaging by MALDI-TOF MS for lipidomics. *Cytotechnology, 72*, 455–468. https://doi.org/10.1007/s10616-020-00393-9

Braga, P. A. D. C., Eberlin, M. N., & Reyes, F. G. R. (2019). Applicability of MALDI-TOF MS for determination of quinolone residues in fish. *Journal of Mass Spectrometry, 12*(54), 1008–1012. https://doi.org/10.1002/jms.4468

Chang, K., Ko, Y. Y., Chou, P. Y., Lai, S. H., & Wang, Y. S. (2024). MAXTOF: An efficient calculation tool for precise optimization of MALDI-TOF MS measurements in real

time. *Journal of The Chinese Chemical Society, 71*. https://doi.org/10.1002/jccs.202400124, 932–341.
Chen, J., Zhao, S., Wesseling, S., Kramer, N. I., Rietjens, I. M. C. M., & Bouwmeester, H. (2023). Acetylcholinesterase inhibition in rats and humans following acute Fenitrothion exposure predicted by physiologically based kinetic modeling-facilitated quantitative in vitro to in vivo extrapolation. *Environmental Science & Technology, 57*(49), 20521–20531. https://doi.org/10.1021/acs.est.3c07077
Deegan, R. D., Bakajin, O., Dupont, T. F., Huber, G., Nagel, S. R., & Witten, T. A. (1997). Capillary flow as the cause of ring stains from dried liquid drops. *Nature, 389*, 827–829. https://doi.org/10.1038/39827
Deegan, R. D., Bakajin, O., Dupont, T. F., Huber, G., Nagel, S. R., & Witten, T. A. (2000). Contact line deposits in an evaporating drop. *Physical Review E, 62*, 756–765. https://doi.org/10.1103/PhysRevE.62.756
Deininger, S. O., Cornett, D. S., Paape, R., Becker, M., Pineau, C., Rauser, S., … Wolski, E. (2011). Normalization in MALDI-TOF imaging datasets of proteins: Practical considerations. *Analytical and Bioanalytical Chemistry, 401*, 167–181. https://doi.org/10.1007/s00216-011-4929-z
Dolinová, J., Klánová, J., Klán, P., & Holoubek, I. (2004). Photodegradation of organic pollutants on the spruce needle wax surface under laboratory conditions. *Chemosphere, 57*(10), 1399–1407. https://doi.org/10.1016/j.chemosphere.2004.09.009
Dreisewerd, K., Schürenberg, M., Karas, M., & Hillenkamp, F. (1995). Influence of the laser intensity and spot size on the desorption of molecules and ions in matrix-assisted laser desorption/ionization with a uniform beam profile. *International Journal of Mass Spectrometry and Ion Processes, 141*(2), 127–148. https://doi.org/10.1016/0168-1176(94)04108-J
Feng, C., Xu, Q., Qiu, X., Jin, Y., Ji, J., Lin, J., Le, S., Wang, G., & Lu, D. (2020). Comprehensive strategy for analysis of pesticide multi-residues in food by GC-MS/MS and UPLC-Q-Orbitrap. *Food Chemistry, 320*, Article 126576. https://doi.org/10.1016/j.foodchem.2020.126576
Fonville, J. M., Carter, C., Cloarec, O., Nicholson, J. K., Lindon, J. C., Bunch, J., & Holmes, E. (2012). Robust data processing and normalization strategy for MALDI mass spectrometric imaging. *Analytical Chemistry, 84*(3), 1310–1319. https://doi.org/10.1021/ac201767g
Giampà, M., Lissel, M. B., Patschkowski, T., Fuchser, J., Hans, V. H., Gembruch, O., Bednarz, H., & Niehaus, K. (2016). Maleic anhydride proton sponge as a novel MALDI matrix for the visualization of small molecules (<250 m/z) in brain tumors by routine MALDI ToF imaging mass spectrometry. *Chemical Communications, 52*(63), 9801–9804. https://doi.org/10.1039/C6CC02387H
Halle, A., Drncova, D., & Richard, C. (2006). Phototransformation of the herbicide Sulcotrione on maize Cuticular wax. *Environmental Science & Technology, 40*(9), 2989–2995. https://doi.org/10.1021/es052266h
Hejazi, P. B. A. S. H. (2020). Retarding spreading of surfactant drops on solid surfaces: Interplay between the Marangoni effect and capillary flows. *Physical Review Fluids, 5*(8), Article 084006. https://doi.org/10.1103/physrevfluids.5.084006
Hong, M., Yang, X., Zhang, X., Ji, Y., Zhou, L., Xiu, G., Ni, Z., & Richard, C. (2021). Aqueous photodegradation of the benzophenone fungicide metrafenone: Carbon-bromine bond cleavage mechanism. *Water Research, 206*(1), Article 117775. https://doi.org/10.1016/j.watres.2021.117775
Hu, H., & Larson, R. G. (2006). Marangoni effect reverses coffee-ring depositions. *The Journal of Physical Chemistry B, 110*(14), 7090–7094. https://doi.org/10.1021/jp0609232
Kamel, F., & Hoppin, J. A. (2004). Association of pesticide exposure with neurologic dysfunction and disease. *Environmental Health Perspectives, 112*(9), 950–958. https://doi.org/10.1289/ehp.7135
Lepucki, P., Dioguardi, A. P., Karnaushenko, D., Schmidt, O. G., & Grafe, H.-J. (2021). The normalized limit of detection in NMR spectroscopy. *Journal of Magnetic Resonance, 332*, Article 107077. https://doi.org/10.1016/j.jmr.2021.107077
Li, Z. (2022). Modeling plant uptake of organic contaminants by root vegetables: The role of diffusion, xylem, and phloem uptake routes. *Journal of Hazardous Materials, 434*, Article 128911. https://doi.org/10.1016/j.jhazmat.2022.128911
Lux, L., Phal, Y., Hsieh, P.-H., & Bhargava, R. (2022). On the limit of detection in infrared spectroscopic imaging. *Applied Spectroscopy, 76*(1), 105–117. https://doi.org/10.1021/ac2013527
Lv, G., Shan, D., Ma, Y., Zhang, W., Ciren, D., Jiang, S., Dang, B., Zhang, J., Sun, W., & Mao, H. (2024). In-situ quantitative prediction of pesticide residues on plant surface by ATR-FTIR technique coupled with chemometrics. *Spectrochimica Acta Part A: Molecular and Biomolecular Spectroscopy, 305*, Article 123432. https://doi.org/10.1016/j.saa.2023.123432
Maggi, F., Tang, F. H. M., & Tubiello, F. N. (2023). Agricultural pesticide land budget and river discharge to oceans. *Nature, 620*, 1013–1017. https://doi.org/10.1038/s41586-023-06296-x
Monadjemi, S., El Roz, M., Richard, C., & Ter Halle, A. (2011). Photoreduction of Chlorothalonil fungicide on plant leaf models. *Environmental Science & Technology, 45*(22), 9582–9589. https://doi.org/10.1021/es202400s
Ouyang, D., Fu, Z., Li, G., Zhong, C., Yuan, J., Huang, H., … Lin, Z. (2023). Metal-organic framework nanofilm enhances serum metabolic profiles for diagnosis and subtype of cardiovascular disease. *Chinese Chemical Letters, 34*(06), Article 107992. https://doi.org/10.1016/j.cclet.2022.107992
Ouyang, D., Huang, H., He, Y., Chen, J., Lin, J., Chen, Z., Cai, Z., & Lin, Z. (2024). Utilization of hydralazine as a reactive matrix for enhanced detection and on-MALDI-target derivatization of saccharides. *Chinese Chemical Letters, 35*(5), 10885. https://doi.org/10.1016/j.cclet.2023.108885
Ouyang, D., Wang, C., Zhong, C., Lin, J., Xu, G., Wang, G., & Lin, Z. (2024). Organic metal chalcogenide-assisted metabolic molecular diagnosis of 33central precocious puberty. *Chemical Science, 15*, 278–284. https://doi.org/10.1039/d3sc05633c
Pang, G., Chang, Q., Bai, R., Fan, C., Zhang, Z., Yan, H., & Wu, X. (2020). Simultaneous screening of 733 pesticide residues in fruits and vegetables by a GC/LC-Q-TOFMS combination technique. *Engineering, 6*, 432–441. https://doi.org/10.1016/j.eng.2019.08.008
Pimmata, P., Reungsang, A., & Plangklang, P. (2013). Comparative bioremediation of carbofuran contaminated soil by natural attenuation, bioaugmentation and biostimulation. *International Biodeterioration & Biodegradation, 85*, 196–204. https://doi.org/10.1016/j.ibiod.2013.07.009
Rani, L., Thapa, K., Kanojia, N., Sharma, N., Singh, S., Grewal, A. S., Srivastav, A. L., & Kaushal, J. (2021). An extensive review on the consequences of chemical pesticides on human health and environment. *Journal of Cleaner Production, 283*, Article 124657. https://doi.org/10.1016/j.jclepro.2020.124657
Ridha, R. K., Alasady, D. H., Azooz, E. A., & Mortada, W. I. (2024). Rapid synergistic cloud point extraction based on hydrophobic deep eutectic solvent combined with hydride generation atomic absorption spectrometry for determination of selenium in tea samples. *Journal of Food Composition and Analysis, 132*, Article 106286. https://doi.org/10.1016/j.jfca.2024.106286
Semysim, F. A., Ridha, R. K., Azooz, E. A., & Snigur, D. (2024). Switchable hydrophilicity solvent-assisted solidified floating organic drop microextraction for separation and determination of arsenic in water and fish samples. *Talanta, 272*, Article 125782. https://doi.org/10.1016/j.talanta.2024.125782
Shao, Y., Li, Y., Jiang, L., Pan, J., He, Y., & Dou, X. (2016). Identification of pesticide varieties by detecting characteristics of Chlorella pyrenoidosa using visible/near infrared hyperspectral imaging and Raman microspectroscopy technology. *Water Research, 104*, 432–440. https://doi.org/10.1016/j.watres.2016.08.042
Song, Z., Gao, H., Xie, W., Sun, Q., Liang, K., & Li, Y. (2021). Quantitative MALDI-MS assay of steroid hormones in plasma based on hydroxylamine derivatization. *Analytical Biochemistry, 616*, Article 114089. https://doi.org/10.1016/j.ab.2020.114089
Trivella, A., & Richard, C. (2014). New insights into pesticide photoprotection. *Environmental Science and Pollution Research, 21*, 4828–4836. https://doi.org/10.1007/s11356-013-1490-7
Vicente, J., Lavín, Á., Holgado, M., Laguna, M. F., Casquel, R., Santamaría, B., Quintero, S., Hernández, A. L., & Ramírez, Y. (2020). The uncertainty and limit of detection in biosensors from immunoassays. *Measurement Science and Technology, 31*, Article 4, 044004 https://doi.org/10.1088/1361-6501/ab49ec.
Villanueva, E., Glorio-Paulet, P., Giusti, M. M., Sigurdson, G. T., Yao, S., & Rodríguez-Saona, L. E. (2023). Screening for pesticide residues in cocoa (*Theobroma cacao* L.) by portable infrared spectroscopy. *Talanta, 257*, Article 124386. https://doi.org/10.1016/j.talanta.2023.124386
Wang, M., Tian, Q., Li, H., Dai, L., Wan, Y., Wang, M., Han, B., Huang, H., Zhang, Y., & Chen, J. (2023). Visualization and metabolome for the migration and distribution behavior of pesticides residue in after-ripening of banana. *Journal of Hazardous Materials, 446*, Article 130665. https://doi.org/10.1016/j.jhazmat.2022.130665
Wang, T., Wang, S., Cheng, Z., Wei, J., Yang, L., Zhong, Z., Hu, H., Wang, Y., Zhou, B., & Li, P. (2021). Emerging core-shell nanostructures for surface-enhanced Raman scattering (SERS) detection of pesticide residue. *Chemical Engineering Journal, 424*, Article 130323. https://doi.org/10.1016/j.cej.2021.130323
Wang, X., Han, J., Chou, A., Yang, J., Pan, J., & Borchers, C. H. (2013). Hydroxyflavones as a new family of matrices for MALDI tissue imaging. *Analytical Chemistry, 85*(15), 7566–7573. https://doi.org/10.1021/ac401595a
Wang, Z., Li, S., Hu, P., Dai, R., Wu, B., Yang, L., Huang, Y., & Zhuang, G. (2022). Recent developments in the spectrometry of fluorescence, ultraviolet visible and surface-enhanced Raman scattering for pesticide residue detection. *Bulletin of Materials Science, 45*, 202. https://doi.org/10.1007/s12034-022-02774-6
Xu, H., Li, Y., Lu, J., Lu, J., Zhou, L., Chovelon, J.-M., & Ji, Y. (2021). Aqueous photodecomposition of the emerging brominated flame retardant tetrabromobisphenol S (TBBPS). *Environmental Pollution, 271*, Article 116406. https://doi.org/10.1016/j.envpol.2020.116406
Yao, C., Myung, K., Wang, N., & Johnson, A. (2014). Spray retention of crop protection agrochemicals on the plant surface. *Retention, Uptake, and Translocation of Agrochemicals in Plants: American Chemical Society*. https://doi.org/10.1021/bk-2014-1171.ch001
Zhang, M., Xue, J., Li, Y., Yin, Y., Liu, Y., Wang, L., & Li, Z. (2023). Non-destructive detection and recognition of pesticide residue levels on cauliflowers using visible/near-infrared spectroscopy combined with chemometrics. *Food Science, 88*, 4327–4342. https://doi.org/10.1111/1750-3841.16728
Zhao, M., Wu, J., Figueiredo, D. M., Zhang, Y., Zou, Z., Cao, Y., Li, J., Chen, X., Shi, S., Wei, Z., Li, J., Zhang, H., Zhao, E., Geissen, V., Ritsema, C. J., Liu, X., Han, J., & Wang, K. (2023). Spatial-temporal distribution and potential risk of pesticides in ambient air in the North China Plain. *Environment International, 182*, Article 108342. https://doi.org/10.1016/j.envint.2023.108342